Supplementary Material for A Computational Study of the Electronic Properties, Ionic Conduction, and Thermal Expansion of $Sm_{1-x}A_xCoO_3$ and $Sm_{1-x}A_xCoO_{3-x/2}$ (A=Ba^{2+}, Ca^{2+}, Sr^{2+}, and x=0.25, 0.5) as Intermediate Temperature SOFC Cathodes

Emilia Olsson, [1] *Xavier Aparicio-Anglès,* [1] *and Nora H. de Leeuw.*[1, 2*]

1 Department of Chemistry, University College London, London, WC1H 0AJ, United Kingdom

2 School of Chemistry, Cardiff University, Main Building, Park Place, Cardiff, CF10 3AT, United Kingdom

The Electronic Supporting Information contains calculated and experimental lattice parameters for cubic and orthorhombic $SmCoO_3$, as well as Sm_2O_3 using interatomic potentials (table S1), a description of the Goldschmidt factor and its calculated values (table S2), the relative energies between the different dopant configurations (table S3), lattice parameters, and interatomic distances in dopant systems for the most stable configuration (table S4), and a discussion of the solution energy (table S5). Furthermore, graphical representations of all oxygen vacancy-dopant configurations and their oxygen vacancy formation energies are included in figures S1-4. In tables S6 and S7, Bader charges have been collected, and mean square displacement plots are presented in figures S4 and S5. Table S8 contains all diffusion coefficients used to calculate ionic conductivity and activation energies.

Table S1. Calculated and experimental lattice parameters for cubic and orthorhombic $SmCoO_3$, as well as Sm_2O_3 using interatomic potentials.

	Calculated lattice parameters (Å)	**Experimental lattice parameters (Å)**	**Difference (%)**
Cubic	3.75	3.75	0.0
Orthorhombic	5.30, 5.34, 7.51	5.28, 5.35, 7.50	0.37, 0.19, 0.09
Sm_2O_3	10.68	10.85	1.53

Goldschmidt Tolerance Factor

The Goldschmidt tolerance factor (t) is commonly used to indicate perovskite stability, and can be used to calculate the most favorable lattice site for a dopant to substitute at (eq. 1).[1,2]

$$t = \frac{r_A + r_O}{\sqrt{2}(r_B + r_O)} \quad (1)$$

where r_A, r_B, and r_O, are the ionic radii of the *A*-, and *B*-site atom, and oxygen. Ideally, t=1 for perovskites ($t^{SmCoO_3} = 0.96$). Thus, the site with t closest to 1 is the most favorable for this substitution. The results are presented below, with all the dopants studied here preferably substituting at the Sm-site.

Table S2. Goldschmidt tolerance factor for different dopants in $SmCoO_3$. Undoped has tolerance factor of 0.96.

Dopant	t^{Sm}	t^{Co}
Ca	0.94	0.70
Sr	1.01	0.65
Ba	1.07	0.61

Dopant Configuration

When x = 0.25, configuration 1 is the most stable for all three dopants, and the range of energies is about 1.0 eV, with the other configurations found at least 0.4 eV higher in energy than the most stable structure, regardless of dopant. On the other hand, for x=0.50, configuration 3 is the most stable for Ba^{2+} and Sr^{2+}, whereas for Ca^{2+} configuration 4 is the most stable. At this concentration, the range of energies is larger compared to x=0.25; for Ca^{2+} the range is 3.5 eV, for Sr^{2+} 1.7 eV, and 5.2 eV for Ba^{2+}, and the difference in energies between the most stable configuration and the next one is between 0.5 and 0.7 eV for the different dopants. A full list of relative energies is included in table S3. Furthermore, introducing dopants on the Sm-site leads to increased lattice volume in the pseudocubic structure, as found from DFT+U calculations. Deviations from the perfect cubic lattice are observed, with disorder present in the Sm-O and Co-O bonds (table S4).

Table S3. Energy differences (eV) for dopant configurations. Numbers refer to SOD configuration.

	Ca		**Sr**		**Ba**	
	x=0.25	x=0.5	x=0.25	x=0.5	x=0.25	x=0.5
1	0.0	1.6	0.0	0.7	0.0	0.4
2	0.4	3.5	0.9	1.7	0.9	1.4
3	1.1	0.5	1.2	0.0	0.8	0.0
4		0.0		0.5		0.8
5		1.4		0.7		0.7
6		4.3		4.0		5.2

Table S4. Volumes (Å^3) and interatomic distances in dopant systems for the most stable configuration (N) referring to figure S1. A refers to dopant.

System	N	Volume	Sm-O	Co-O	A-O
$SmCoO_3$[3]		52.73	2.65	1.88	N/A
$Sm_{0.75}Ca_{0.25}CoO_3$	1	54.43	2.60-2.69	1.89, 1.91	2.74, 2.76
$Sm_{0.50}Ca_{0.50}CoO_3$	4	54.01	2.69-3.03	1.91-1.95	2.69-2.95
$Sm_{0.75}Sr_{0.25}CoO_3$	1	54.58	2.58-2.73	1.89-1.92	2.77, 2.80
$Sm_{0.50}Sr_{0.50}CoO_3$	3	55.59	2.57-2.72	1.91	2.69-2.83
$Sm_{0.75}Ba_{0.25}CoO_3$	1	56.33	2.56-2.77	1.91, 1.96	2.84
$Sm_{0.50}Ba_{0.50}CoO_3$	3	58.41	2.55-2.78	1.92-1.96	2.74-2.92

For the most stable dopant configurations we have explored the non-equivalent V_O positions with SOD and the remaining symmetry operations per system, leading to a total of 39 non-equivalent V_O distributions. Low V_O concentrations do not have a significant effect on the lattice parameters, [15] and the supercell volume can thus be kept constant when introducing V_O. The most stable dopant-vacancy configurations are presented in ESI figure S1-4.

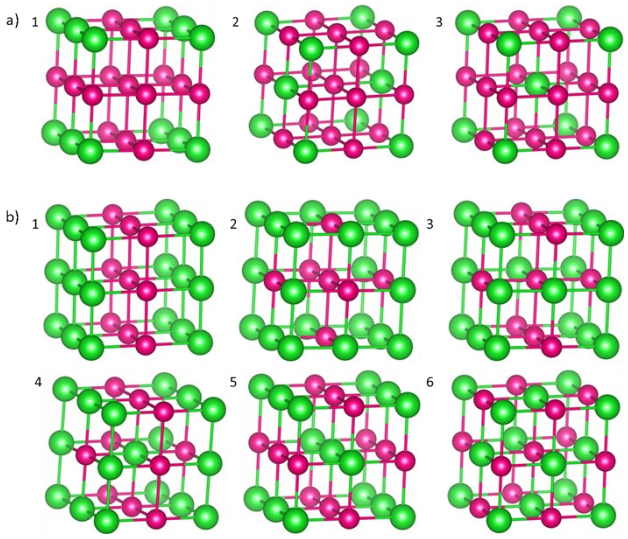

Figure S1. Ball-and-stick representation of the three non-equivalent configurations for a) $Sm_{0.75}A_{0.25}CoO_3$, and the six non-equivalent configurations for b) $Sm_{0.5}A_{0.5}CoO_3$ as calculated with SOD. O and Co have been omitted for clarity. Sm are colored in pink whereas the dopant is colored in green.

Dopant, and oxygen vacancy configuration

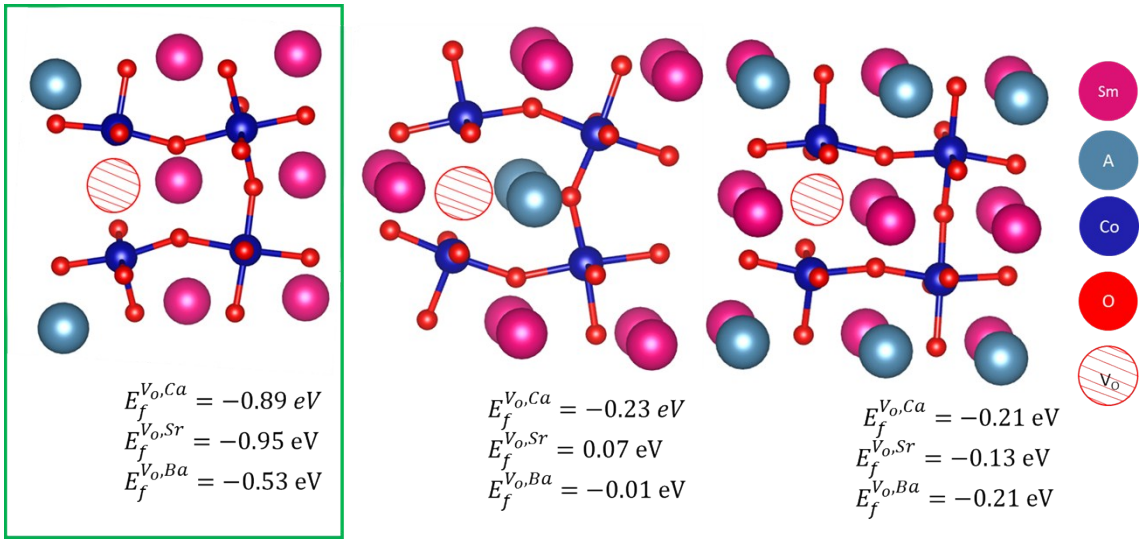

Figure S2. V_O configurations for $Sm_{0.75}A_{0.25}CoO_{2.88}$ with noted E_f. Green rectangle notes lowest E_f.

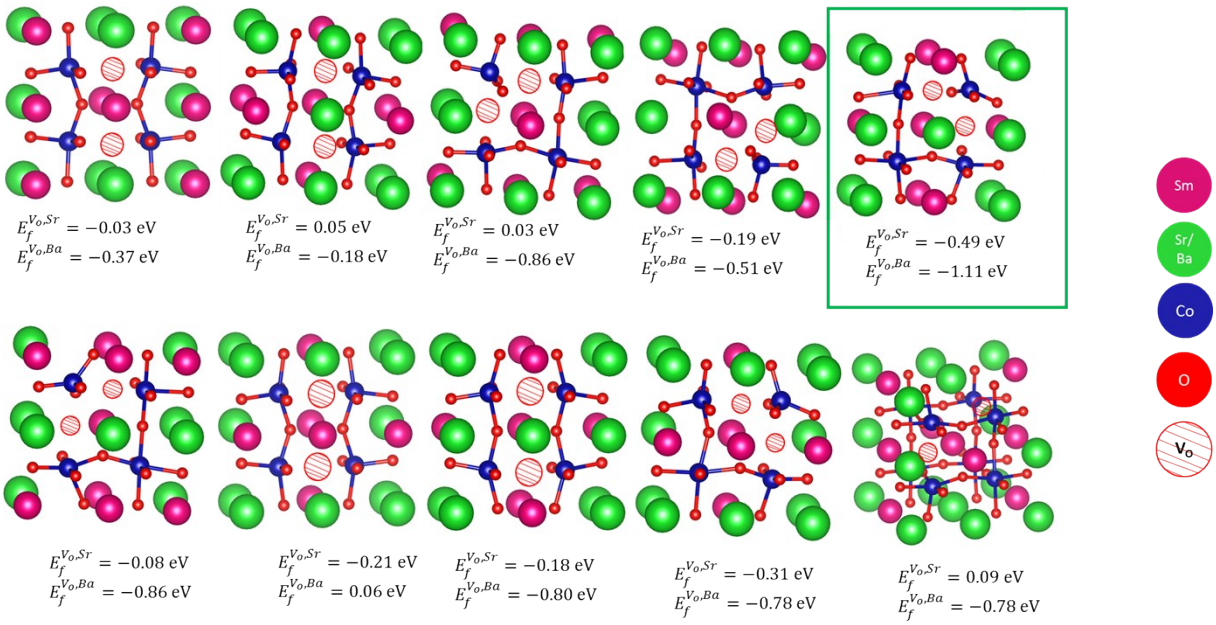

Figure S3. V_O configurations for $Sm_{0.5}A_{025}CoO_{2.75}$ (A=Sr, Ba) with noted E_f. Green rectangle notes lowest E_f.

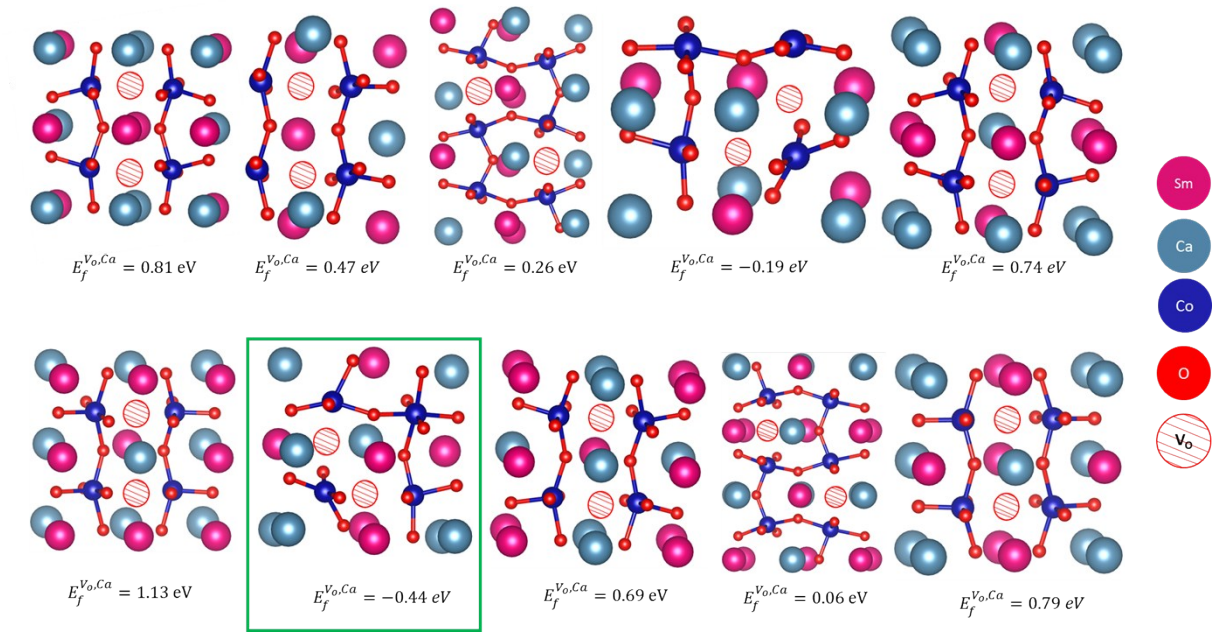

Figure S4. V_O configurations for $Sm_{0.5}Ca_{025}CoO_{2.75}$ with noted E_f. Green rectangle notes lowest E_f.

Solution energy

To calculate the solution energy (E_f), we have employed the method developed by Zhang and Northrup (eq. 2),[4,5]

$$E_f = E_{Defective} - E_{Perfect} + \sum_i n_i \mu_i \qquad \text{eq 2}$$

where $E_{Defective}$ is the total energy of the defective system, $E_{Perfect}$ is the total energy of the non-defective system; n_i is the number of removed or added species *i* from the bulk, and μ_i is the chemical potential of species *i* . The chemical potential of A and Sm have been calculated from the total DFT energy of the respective metals (Sm: -4.62 eV, Ca: -1.93 eV, Sr:-1.64 eV, Ba: -1.91 eV),[3,6] considering a Sm/A rich-regime. The solution energies, *i.e.* the dopant substitution energies, (E_f^A) are collected in table S5. The most favorable solution energy is found for Sr^{2+}.

Table S5. Solution energies (E_f^A)

	E_f^A **(eV)**
Ca_{Sm}	3.46
Sr_{Sm}	3.03
Ba_{Sm}	3.75

Bader Charges

Table S6. Unique Bader charges (q) for fully oxidized $Sm_{1-x}A_xCoO_3$. A is dopant.

System	q_{Sm} (e)	q_O (e)	q_A (e)
$SmCoO_3$[3]	+2.01	-1.11	
$Sm_{0.75}Ba_{0.25}CoO_3$	+2.13, +2.10	-1.11	+1.57
$Sm_{0.50}Ba_{0.50}CoO_3$	+2.12, +2.16	-1.10	+1.40
$Sm_{0.75}Ca_{0.25}CoO_3$	+2.07, +2.17	-1.12	+1.60
$Sm_{0.50}Ca_{0.50}CoO_3$	+2.13, +2.15	-1.07	+1.55, +1.52
$Sm_{0.75}Sr_{0.25}CoO_3$	+2.10, +2.14	-1.11	+1.57
$Sm_{0.50}Sr_{0.50}CoO_3$	+2.08	-1.06	+1.58

Table S7. Bader charges (q) for $Sm_{1-x}A_xCoO_{3-x/2}$. A is dopant.

System	q_{Sm} (e)	q_O (e)	q_A (e)
$SmCoO_3$[3]	+2.01	-1.11	
$Sm_{0.75}Ba_{0.25}CoO_{2.88}$	+2.10	-1.14	+1.60
$Sm_{0.50}Ba_{0.50}CoO_{2.75}$	+2.11	-1.15	+1.58
$Sm_{0.75}Ca_{0.25}CoO_{2.88}$	+2.10	-1.15	+1.54
$Sm_{0.50}Ca_{0.50}CoO_{2.75}$	+2.12	-1.11	+1.52
$Sm_{0.75}Sr_{0.25}CoO_{2.88}$	+2.10	-1.13	+1.58
$Sm_{0.50}Sr_{0.50}CoO_{2.75}$	+2.12	-1.14	+1.58

Oxygen Diffusion

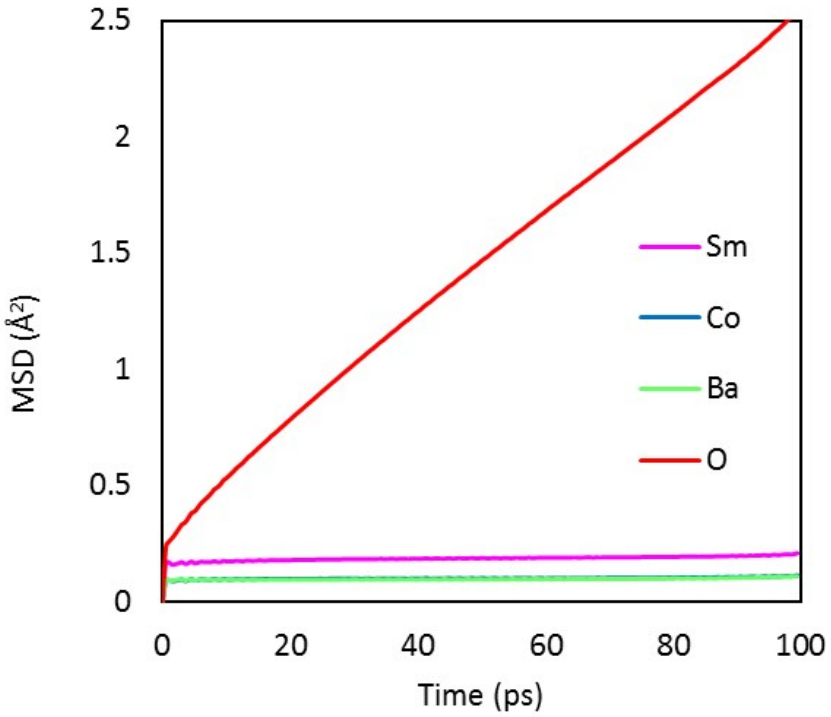

Figure S5. Mean square displacement (MSD) graph for $Sm_{0.75}Ba_{0.25}CoO_{2.88}$ at 1500 K

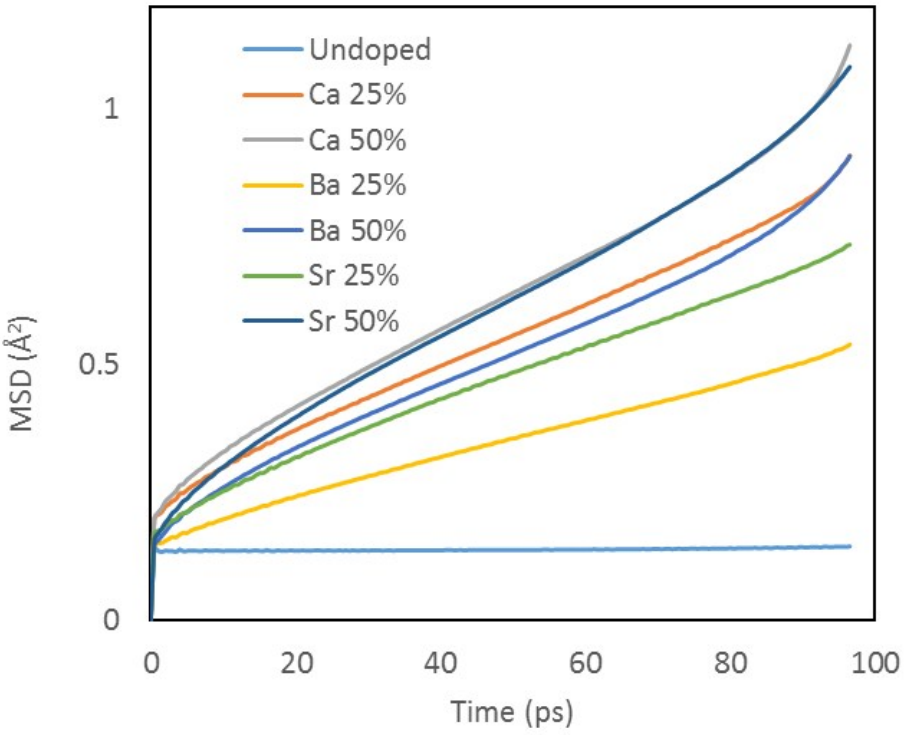

Figure S6. Oxygen ion MSD in doped and undoped $SmCoO_3$ at 1000 K.

Table S8. Oxygen diffusion coefficients (D_O) for the different dopant systems, at two dopant concentrations (x), and different temperatures (T).

System	T (K)	D_O (cm²s⁻¹)	
		x=0.25	x=0.50
$Ba_xSm_{1-x}CoO_{3-x/2}$	800	2.06×10^{-8}	5.52×10^{-8}
	1000	6.63×10^{-8}	1.11×10^{-7}
	1200	1.26×10^{-7}	2.08×10^{-7}
	1500	3.69×10^{-7}	4.83×10^{-7}
$Ca_xSm_{1-x}CoO_{3-x/2}$	800	4.27×10^{-8}	6.68×10^{-8}
	1000	1.10×10^{-7}	1.32×10^{-7}
	1200	2.77×10^{-7}	2.49×10^{-7}
	1500	8.40×10^{-7}	7.46×10^{-7}
$Sr_xSm_{1-x}CoO_{3-x/2}$	800	3.84×10^{-8}	7.03×10^{-8}
	1000	9.70×10^{-8}	1.39×10^{-7}
	1200	2.21×10^{-7}	2.87×10^{-7}
	1500	6.80×10^{-7}	7.73×10^{-7}

References

[1] V.M. Goldschmidt, Naturwissenschaften **14**, 477 (1926).

[2] X.C. Liu, R. Hong, and C. Tian, J. Mater. Sci. Mater. Electron. **20**, 323 (2009).

[3] E. Olsson, X. Aparicio-Anglès, and N.H. De Leeuw, J. Chem. Phys. **145**, 14703 (2016).

[4] S.T. Murphy and N.D.M. Hine, Phys. Rev. B - Condens. Matter Mater. Phys. **87**, 1 (2013).

[5] S. Zhang and J. Northrup, Phys. Rev. Lett. **67**, 2339 (1991).

[6] P.G. Sundell, M.E. Björketun, and G. Wahnström, Phys. Rev. B **73**, 104112 (2006).